Short communication

Methylene ethylene carbonate: Novel additive to improve the high temperature performance of lithium ion batteries

Dinesh Chalasani [a], Jing Li [b], Nicole M. Jackson [b], Martin Payne [b], Brett L. Lucht [a,*]

[a] University of Rhode Island, Department of Chemistry, 51 Upper College Road, Kingston, RI 02881, United States
[b] Novolyte Technologies, 8001 East Pleasant Valley Road, Cleveland, OH 44131, United States

ARTICLE INFO

ABSTRACT

The preparation of methylene ethylene carbonate (MEC) and the incorporation of MEC into lithium ion batteries as an electrolyte additive were investigated. MEC is prepared in good yield by mercury catalyzed cyclization. Addition of low concentrations of MEC (1–2%) to 1 M $LiPF_6$ in 3:7 ethylene carbonate/ethyl methyl carbonate improves the capacity retention of lithium ion batteries cycled at elevated temperature (60 °C). Ex situ surface analysis (XPS and FTIR) of the electrodes supports the presence of poly(methylene ethylene carbonate) on the anode surface. Modification of the anode solid electrolyte interphase (SEI) correlates with significant improvements in the cycling performance at 60 °C.

1. Introduction

Lithium ion batteries are the dominant secondary battery technology for portable electronic applications and there is great interest in the use of lithium ion batteries in electric vehicle (EV) applications. However, the performance requirements are much more stringent for EV application compared to portable electronics applications. EV applications require longer life and greater operational and survival temperature ranges. The more stringent requirements are often limited by the performance of the electrolyte [1]. In particular, the high temperature performance and calendar life are typically limited by the thermal stability of the electrolyte and reactions of the electrolyte with the protective anode solid electrolyte interphase (SEI) [2–4].

One method for improving the calendar life and high temperature stability of lithium ion batteries is the incorporation of additives which are sacrificially reduced on the surface of the anode to generate a more stable anode SEI. The most widely used additive in lithium ion batteries is vinylene carbonate (VC). Incorporation of VC into lithium ion batteries has been reported to improve cycling stability at elevated temperature (>50 °C) [5–9]. Investigations into the source of performance improvements suggest that VC reacts on the surface of both the graphite anode and metal oxide cathode. However, the generation of poly(alkyl carbonate) on the graphite surface is typically cited as the primary source of performance enhancements.

In this manuscript, we report a novel anode SEI film forming additive, methylene ethylene carbonate (MEC) [10,11]. MEC is readily synthesized via a mercury catalyzed cyclization reaction [12]. Incorporation of MEC into lithium ion cells results in a significant improvement in capacity retention upon cycling at elevated temperature (60 °C). Ex situ surface analysis of the electrodes suggests that poly(methylene ethylene carbonate) is generated on the anode and cathode surfaces and is the likely source for performance enhancements. MEC is a promising thermal stabilizing additive for lithium ion batteries.

2. Experimental

All of the materials for the synthesis of MEC were purchased from Sigma Aldrich or Acros and used without further purification. Battery grade ethyl methyl carbonate (EMC), dimethyl carbonate (DMC), diethyl carbonate (DEC), and lithium hexafluorophosphate ($LiPF_6$) were provided by Novolyte and used without further purification. MEC is purified by recrystallization and its purity is assessed from ^{1}H and ^{13}C NMR spectroscopy and gas chromatography. Prismatic cells (650 mAh) containing an artificial graphite anode and a $LiNi_{1/3}Mn_{1/3}Co_{1/3}O_2$ cathode were prepared with 1 M $LiPF_6$ in EC:EMC (3:7 by volume) with and without added MEC. Related lithium ion coin cells are prepared with 1 M $LiPF_6$ in 1:1:1 EC:EMC:DEC with and without 2% (wt) added MEC. The coin cells used for testing the electrolyte formulations contained $LiNi_{0.8}Co_{0.2}O_2$ (LNCO) as the active cathode material and

* Corresponding author. Tel.: +1 401 874 5071; fax: +1 401 874 5071.
E-mail address: blucht@chm.uri.edu (B.L. Lucht).

mesocarbon microbeads (MCMB) graphite as the active anode material. The coin cells contained 30 μL electrolyte and polyethylene film for a separator and were used for the ex situ surface analysis of the electrodes. The coin cells were cycled with a constant current-constant voltage charge and a constant current discharge between 4.1 V and 3.0 V using a battery cycler (BT-2000 Arbin cycler, College Station, TX). The cells were cycled with the following formation procedures: first cycle at C/20, second and third cycle at C/10 and remaining two cycles at C/5. After the initial five formation cycles the cells were cycled at C/5 rate at room temperature.

2.1. Synthesis of t-BOC protected propargyl alcohol (Eq. (1))

To a solution of propargyl alcohol 20 g (0.356 mol) in 30 mL methylene chloride are added N,N-diisopropylethyl amine 115.0 g (0.89 mol) and dimethyl amino pyridine 4.34 g (0.0356 mol) at room temperature under nitrogen. The contents are stirred in an ice bath while di-t-butyl dicarbonate 100 g (0.462 mol) is slowly added under nitrogen purge. The reaction mixture is allowed to stir for 3 h as the ice bath warms to room temperature. The reaction mixture is then washed with water, 10% HCl solution, 10% NaHCO$_3$ solution, and NaCl solution (150 mL each) followed by drying with
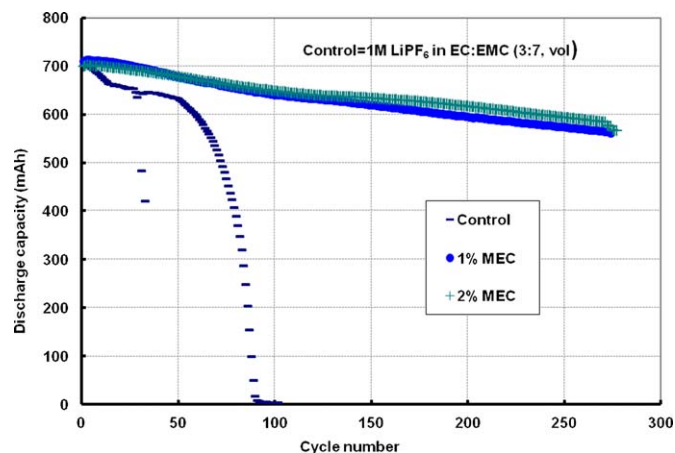

Fig. 1. Discharge capacity vs. cycle number for Li[Ni$_{1/3}$Co$_{1/3}$Mn$_{1/3}$]O$_2$-based cells containing 1 M LiPF$_6$ in 3:7 EC/EMC with and without added MEC. The cells were cycled at 1C rate between 3.0 and 4.2 V at 60 °C.
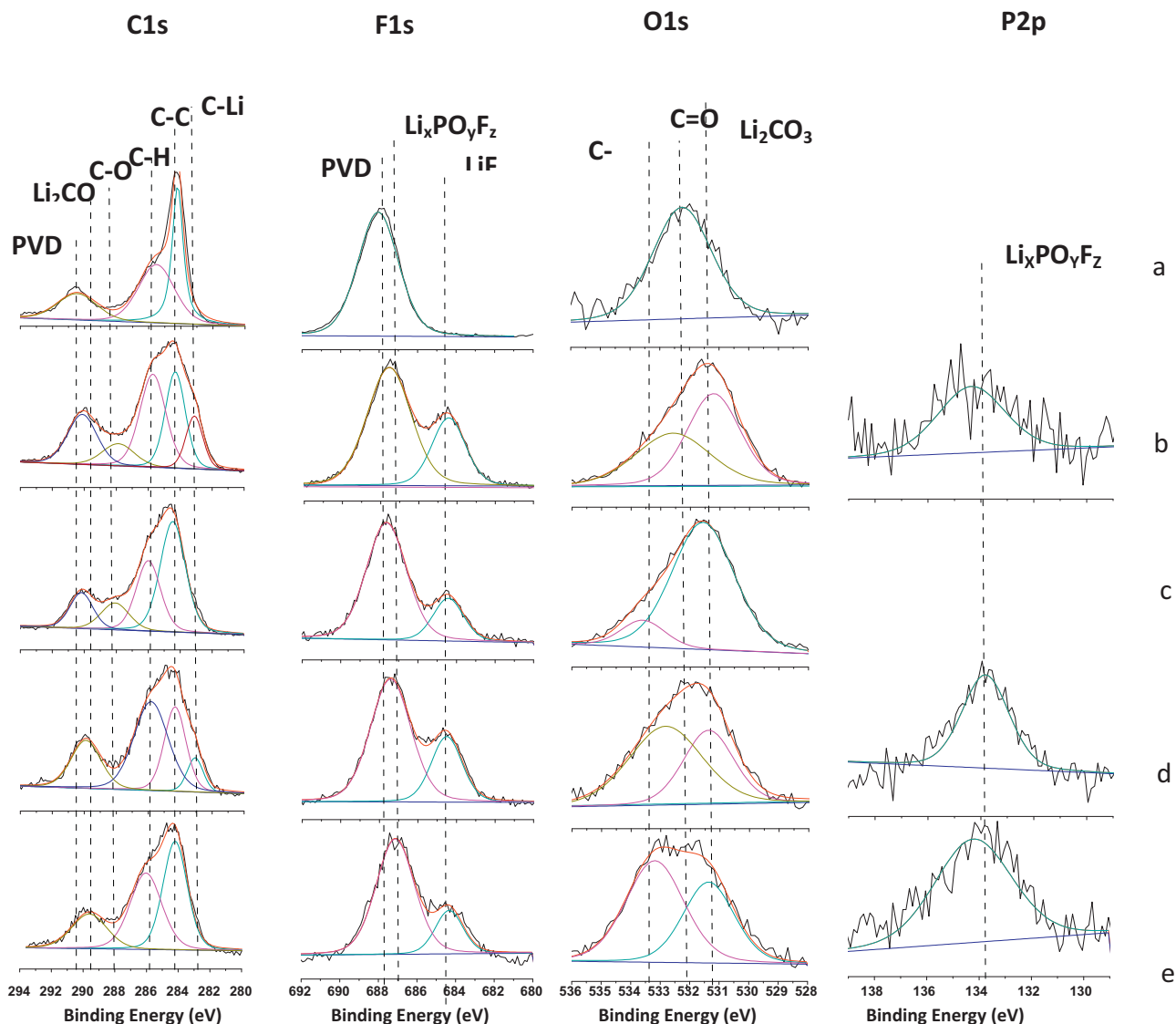

Fig. 2. XPS spectra of anodes (a) fresh uncycled anode; (b) 1 M LiPF$_6$ in EC:EMC:DEC (1:1:1) after formation cycling; (c) 1 M LiPF$_6$ in EC:EMC:DEC (1:1:1) +2% MEC after formation cycling; (d) 1 M LiPF$_6$ in EC:EMC:DEC after cycling and storage at 60 °C; (e) 1 M LiPF$_6$ in EC:EMC:DEC (1:1:1) +2% MEC after cycling and storage at 60 °C.

Fig. 3. XPS spectra of cathodes (a) fresh uncycled cathode; (b) 1 M LiPF6 in EC:EMC:DEC (1:1:1) after formation cycling; (c) 1 M LiPF$_6$ in EC:EMC:DEC (1:1:1) +2% MEC after formation cycling; (d) 1 M LiPF$_6$ in EC:EMC:DEC after cycling and storage at 60 °C; (e) 1 M LiPF$_6$ in EC:EMC:DEC (1:1:1) +2% MEC after cycling and storage at 60 °C.
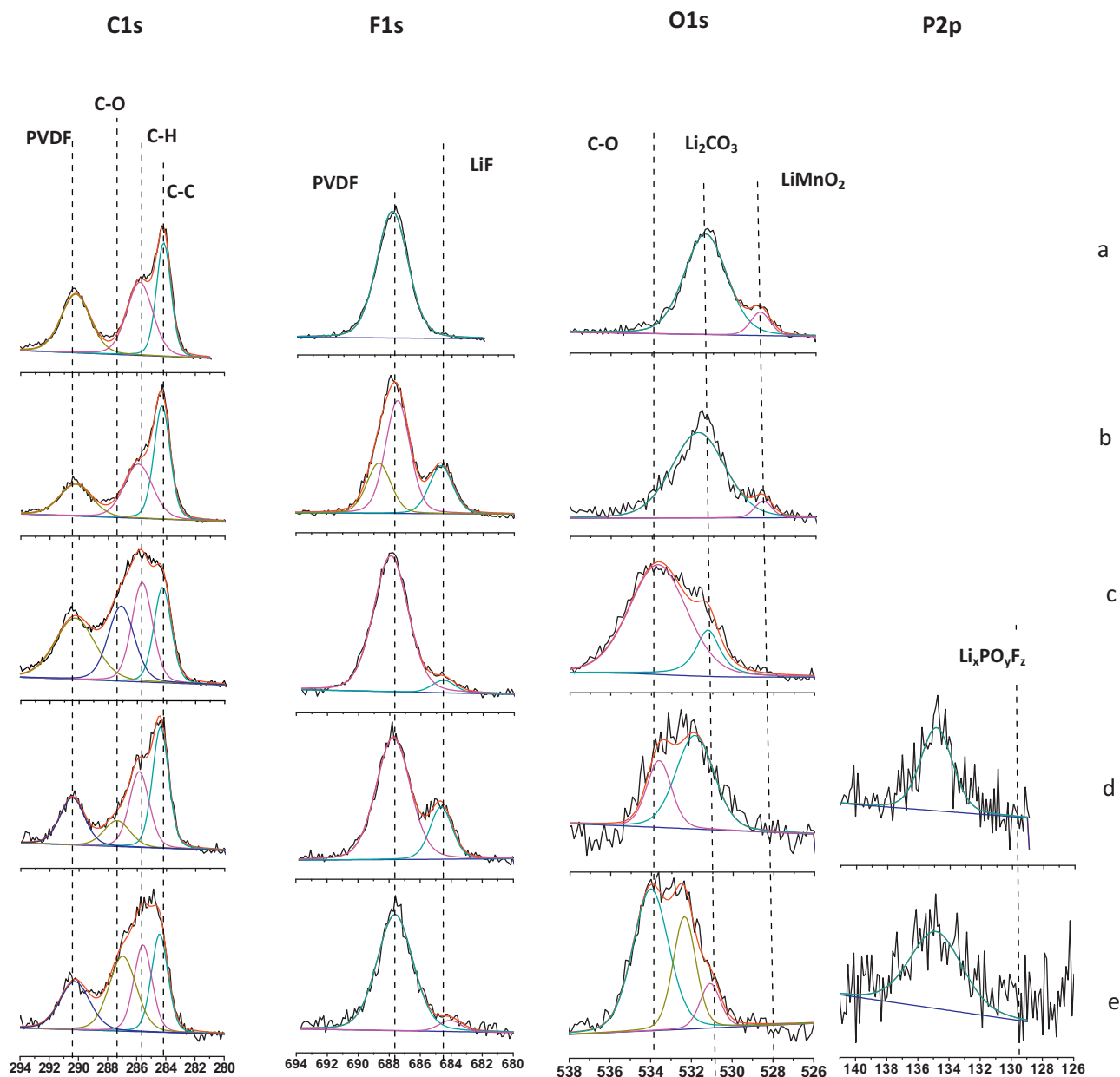
magnesium sulfate. The residual solvent is removed via rotary evaporation to yield the *t*-BOC propargyl alcohol (52.8 g, 95% yield).

2.2. Synthesis of MEC (Eq. (1)): **1**

A suspension of mercury (II) triflate 6.36 g (12.7 mmol) and tetra methyl urea 4.44 g (38.07 mmol) in 150 mL methylene chloride is stirred for 30 min in a round bottom flask in a nitrogen filled glove box. To that suspension is added *t*-BOC propargyl alcohol

40 g (0.256 mol) and stirred over night. The contents are filtered through silica gel to remove the mercury salts and tetra methyl urea. The residual solvent is removed via rotary evaporation followed by recrystallization in pentane to yield MEC (11.5 g, 45% yield). The purity of MEC as estimated by NMR spectroscopy is >99%. ^{1}H NMR (300 MHz, CDCl$_3$) δ 4.95 (t, 2H), 4.79 (m, 1H), 4.38 (m, 1H). ^{13}C NMR (75 MHz, CDCl$_3$) δ 152.83, 148.93, 67.60, 87.00. Melting point: 31–33 °C.
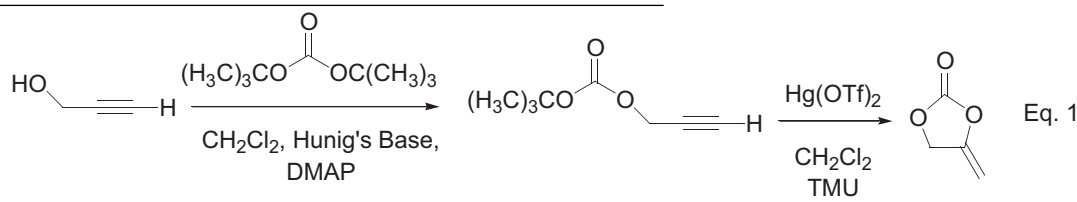
(1)

Fig. 4. FTIR spectra of anodes (a) fresh uncycled anode; (b) 1 M LiPF6 in EC:EMC:DEC (1:1:1) after formation cycling; (c) 1 M $LiPF_6$ in EC:EMC:DEC (1:1:1) +2% MEC after formation cycling; (d) 1 M $LiPF_6$ in EC:EMC:DEC after cycling and storage at 60 °C; (e) 1 M $LiPF_6$ in EC:EMC:DEC (1:1:1) +2% MEC after cycling and storage at 60 °C.
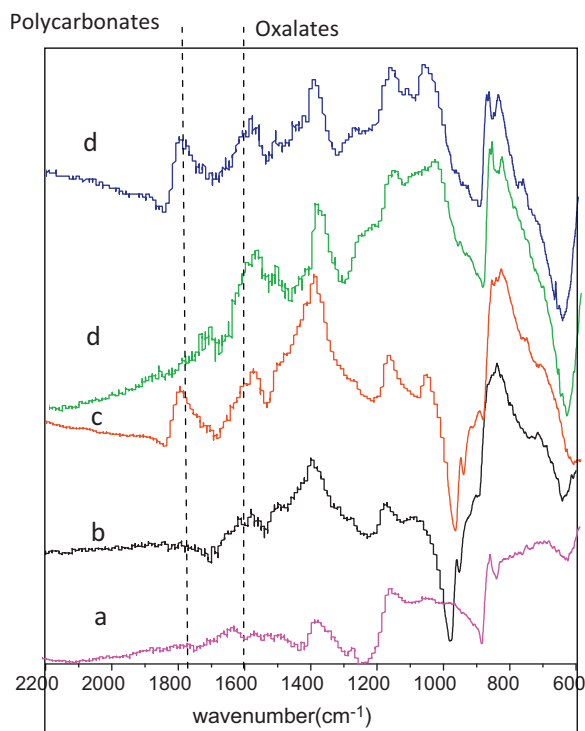

Fig. 5. FTIR spectra of cathodes (a) fresh uncycled anode; (b) 1 M $LiPF_6$ in EC:EMC:DEC (1:1:1) after formation cycling; (c) 1 M $LiPF_6$ in EC:EMC:DEC (1:1:1) +2% MEC after formation cycling; (d) 1 M $LiPF_6$ in EC:EMC:DEC after cycling and storage at 60 °C; (e) 1 M $LiPF_6$ in EC:EMC:DEC (1:1:1) +2% MEC after cycling and storage at 60 °C.
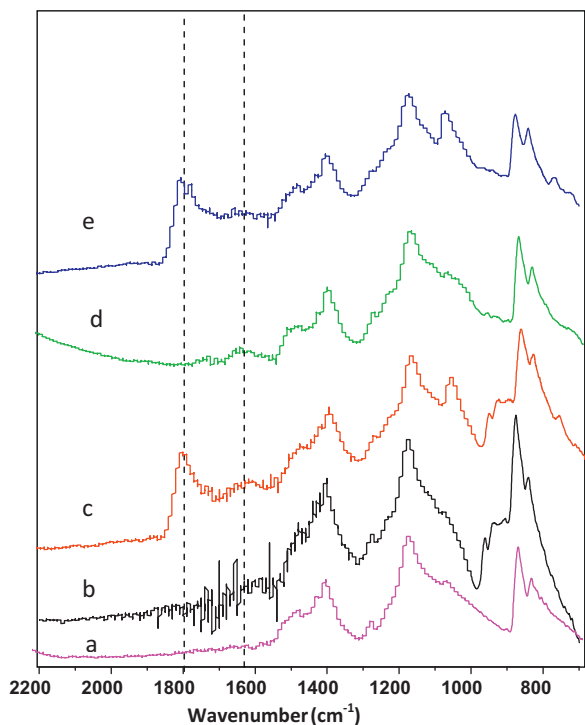
The cells were opened in an Ar glove box after cycling and the electrodes were extracted for surface analysis. The electrodes were rinsed with dimethyl carbonate (DMC) three times prior to surface analysis. The XPS spectra were acquired with a PHI 5500 system using Al Kα radiation ($h\nu$ = 1486.6 eV) under ultra high vacuum. Characterization of XPS peaks was made by recording XPS spectra for reference compounds, which would be present on the electrode surfaces: LiF, Li_2CO_3, $Li_xPO_yF_z$ and lithium alkylcarbonate. The graphite peak at 284.3 eV was used as a reference for the final adjustment of the energy scale in the spectra. Lithium was not monitored due to its low inherent sensitivity and small change of binding energy. The spectra obtained were analyzed by Multipak 6.1A software and fitted using XPS peak software (version 4.1). A mixture of Lorentzian and Gaussian functions was used for the least-squares curves fitting procedure. Scanning electron microscopy (SEM) images were taken on a JEOL 5900 scanning electron microscope. Fourier transfer infrared spectroscopy (FTIR) was conducted on a Thermo Scientific Nicolet iS10 Spectrometer with an attenuated total reflection (ATR) accessory. The spectra were acquired with a resolution of 4 cm^{-1} and a total of 128 scans.

3. Results and discussion

3.1. Electrochemical testing on full cells

The performance of MEC as a thermal stabilizing additive in full cells was examined in 650 mAh prismatic cells containing an artificial graphite anode, $LiNi_{1/3}Mn_{1/3}Co_{1/3}O_2$ cathode, and 1 M $LiPF_6$ electrolyte in EC:EMC (3:7 by volume) with and without added MEC. After typical cell formation cycling at room temperature, the cells were cycled at a 1 C rate between 3.0 and 4.2 V at 60 °C to simulate accelerated aging (Fig. 1). Cells containing 1 or 2% of MEC have outstanding capacity retention (∼80%) after 270 cycles at 60 °C. Comparable cells containing standard electrolyte failed after less than 100 cycles at 60 °C. In order to better understand the source

of the performance enhancement by MEC, related coin cells were cycled and ex situ analysis of the electrodes was conducted. The cycling performance of the coin cells after thermal storage was similar to that observed for the accelerated aging experiments on the 650 mAh cells.

3.2. Surface analysis

The surfaces of three sets of electrodes were analyzed by X-ray photo electron spectroscopy (XPS), scanning electron microscopy (SEM), and infra-red spectroscopy with attenuated total reflectance (IR-ATR). The electrode samples were: fresh uncycled electrodes, electrodes after five formation cycles, and electrodes from cells with 30 cycles that were further stored at 60 °C for one week to simulate accelerated aging. The cells were dismantled at a full state of charge in an argon glove box and the anodes and cathodes were extracted. The electrodes were washed with DMC and dried under vacuum.

3.3. XPS analysis

The electrodes were analyzed by XPS. Figs. 2 and 3 contain XPS spectra of the anodes and cathodes while the elemental concentrations are summarized in Tables 1 and 2. Analysis of the anode surface reveals that the concentration of carbon is decreased and the concentration of oxygen is increased after cycling for both the standard electrolyte and the electrolyte with added MEC consistent with the formation of a solid electrolyte interphase (SEI). Anodes extracted from cells after formation cycling with the standard

Table 1
Elemental composition of C, F, O, and P on anodes.

	C1s%	F1s%	O1s%	P2p%
Fresh, uncycled	65	32	3	–
1 M LiPF$_6$-formation cycling	47	33	19	1
2% MEC-formation cycling	53	21	26	–
1 M LiPF$_6$ (60 °C)	48	33	17	2
2% MEC (60 °C)	51	22	26	2

Table 2
Elemental composition of C, F, O, P, and Ni on cathodes.

	C1s%	F1s%	O1s%	P2p%	Ni2p%
Fresh, uncycled	43	31	11	–	15
1 M LiPF$_6$-formation cycling	47	29	10	–	14
2% MEC-formation cycling	52	23	16	–	9
1 M LiPF$_6$ (60 °C)	43	31	10	1	15
2% MEC (60 °C)	55	15	21	1	8

electrolyte have slightly lower concentrations of carbon and oxygen and a higher concentration of fluorine than the anodes extracted after formation cycling with the electrolyte containing MEC. The concentration of phosphorus is low for both cycled anodes. After additional cycling and storage at 60 °C there are only small changes to the elemental concentration of the surface. The higher concentrations of C and O and lower concentration of F on the surface of the anode is consistent with a thicker anode SEI covering more of the electrode surface and the PVDF binder.

The C1s spectra of fresh anodes contain peaks characteristic of graphite (284.3 eV) and PVDF (285.5 and 290.3 eV). The corresponding peak characteristic of PVDF is observed in the F1s spectrum (687.8 eV) while the O1s spectrum contains a weak peak attributed to graphite surface oxidation (∼632 eV). Significant changes are observed on the electrode surface by XPS after formation cycling. The anode extracted from the cell cycled with standard electrolyte contains new peaks in the C1s spectrum consistent with the formation of C—O (288.2 eV) and C=O (289.5 eV) containing species
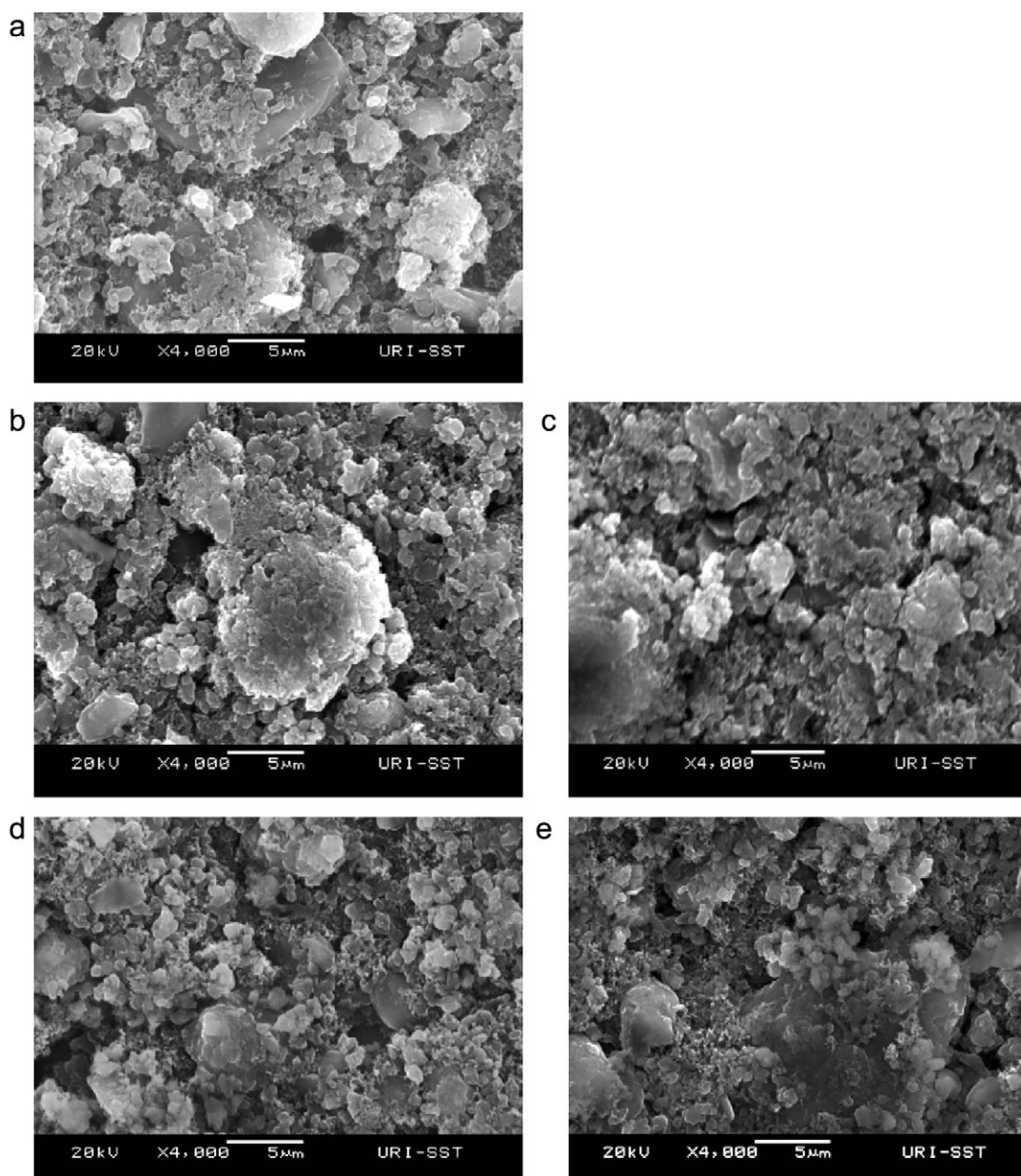
Fig. 6. SEM images of anodes (a) fresh, (b) after formation cycling, (c) after formation cycling with MEC, (d) after cycling and storage, (e) after cycling and storage with MEC.

Fig. 7. SEM images of cathodes (a) fresh, (b) after formation cycling, (c) after formation cycling with MEC, (d) after cycling and storage, (e) after cycling and storage with MEC.
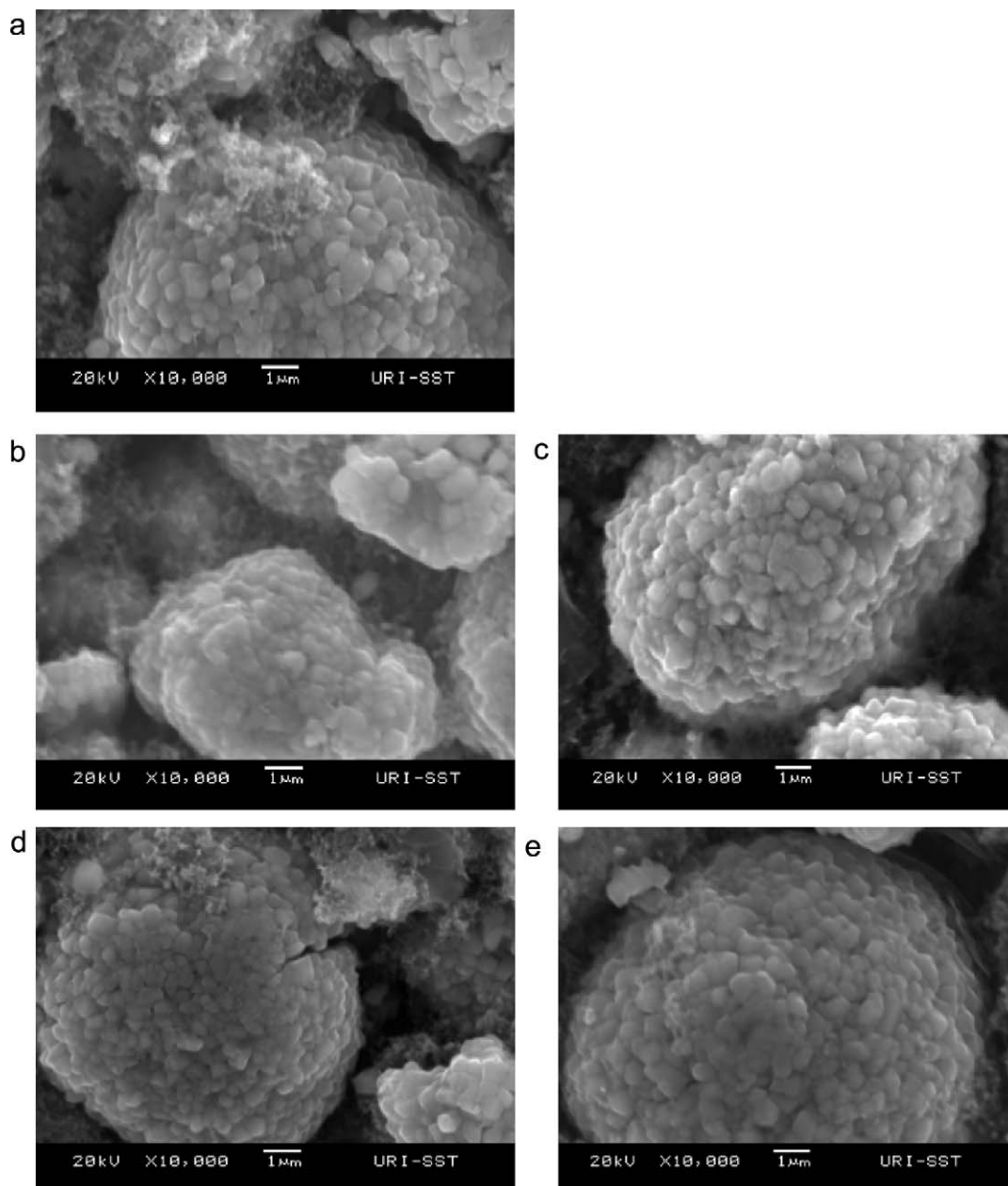
such as lithium alkyl carbonates, lithium alkoxides, and ethers, as previously reported on the anode SEI [8]. In addition, there is a small peak (282.9 eV) characteristic of LiC$_x$. The F1s spectrum contains peaks characteristic of PVDF (687.8 eV) and LiF (684.5 eV). A weak P2p signal is observed for Li$_x$PF$_y$O$_z$ (133.7 eV) while the corresponding F1s peak (687 eV) is similar in binding energy to PVDF. The O1s spectrum contains peaks characteristic of C—O and C=O, consistent with the C1s spectra. Anodes extracted from cells containing MEC after formation cycling have similar XPS spectra to the anodes cycled with standard electrolyte. However, the relative intensity of the peak characteristic of LiF is slightly lower. XPS spectra of the anodes extracted from cells cycled and stored at 60 °C for both electrolytes are similar to the XPS spectra of the anodes after formation cycling suggesting only small changes to the structure of the surface species occur upon aging.

The changes to the cathode surfaces upon cycling were smaller than those observed for the anode surfaces cycled in the presence of standard electrolyte. Analysis of the cathode surfaces after formation cycling with the standard electrolyte suggest very small changes to the concentrations of C, F, O, and Ni. More significant changes were observed for the electrolyte containing MEC. The concentrations of C and O are increased while the concentrations of F and Ni are decreased. This is consistent with the generation of a cathode surface film in the presence of MEC. The elemental concentrations of the cathode surface in both the standard electrolyte and the electrolyte containing MEC do not change significantly upon aging suggesting only small changes to the surface species.

The C1s spectrum of the fresh cathode contains peaks characteristic of graphite (284.3 eV) and PVDF (285.5 and 290.3 eV). The F1s spectrum contains the corresponding PVDF peak (687.8 eV). The O1s spectrum contains peaks characteristic of metal oxide (528 eV) and residual lithium carbonate (531 eV). The cathodes extracted from cells containing standard electrolyte have only small changes after formation cycling. A new small peak characteristic of LiF

is observed (684.5 eV) in the F1s spectrum and the peak in the O1 s spectrum characteristic of metal oxide (528 eV) has decreased intensity. The changes to the surface of the cathode extracted from the cell cycled with electrolyte containing MEC after formation cycles are greater than those observed for the standard electrolyte. New peaks characteristic of C—O containing species including ethers and carbonates are observed (287.5 eV) in the C1s spectrum and (534 eV) in the O1s spectrum. In addition, the peak characteristic of metal oxide (528 eV) is no longer observable suggesting the presence of a relatively thick cathode surface film. Additional cycling and storage at 60 °C results in changes to the surface of the cathode extracted from the cell containing standard electrolyte. Peaks characteristic of C—O and C=O containing species are observed in the C1s and O1s spectra consistent with the formation of lithium alkyl carbonates. The peak of LiF has a slight increase in intensity while the peak of the metal oxide is no longer detectable. In addition, a new peak (136 eV) in the P2p spectrum is observed consistent with the presence of $Li_xPF_yO_z$. Additional cycling and storage at 60 °C results in only small changes to the surface of the cathode cycled in the presence of MEC containing electrolyte. A small peak characteristic of $Li_xPF_yO_z$ is observed in the P2p spectrum.

3.4. FTIR analysis

The IR spectra of both the anodes and cathodes are dominated by peaks from PVDF binder at 1400, 1170, 1070, 877, and 840 cm^{-1} (Fig. 4). The anodes extracted from cells containing standard electrolyte contain a new peak at 1600 cm^{-1} consistent with the presence of oxalates or lithium alkyl carbonates. The anodes of cells cycled with MEC contain the peak characteristic of oxalates and lithium alkyl carbonates along with an additional peak at 1750 cm^{-1} which is characteristic of polycarbonates. The cathodes extracted from cells containing the standard electrolyte have no new absorptions (Fig. 5). However, the cathodes extracted from cells cycled with MEC containing electrolyte have an additional peak at ~1800 cm^{-1} consistent with the presence of polycarbonates.

3.5. SEM analysis

SEM analysis of the fresh anode materials reveal MCMB particles ranging in size from 0.5 to 5 μm diameter (Fig. 6). After formation cycling the surface of the MCMB particles appears to be coated with a surface film for both the standard electrolyte and the electrolyte containing MEC. The appearance of this surface film is similar for both electrolytes. SEM images of the anodes after thermal storage and cycling appear to have additional surface film coverage for both the standard and MEC containing electrolytes. However, the surface films appear similar for both electrolytes. SEM analysis of the cathodes before cycling, after formation cycling, and after storage at elevated temperature with cycling are very similar suggesting that any surface films on the cycled cathodes are very thin (Fig. 7).

4. Summary

A novel anode SEI film forming additive, methylene ethylene carbonate (MEC), has been reported. MEC is prepared in good yield and purity by mercury catalyzed cyclization. Addition of low concentrations of MEC (1–2%) to commercial lithium ion battery electrolytes ($LiPF_6$ in carbonates) improves the capacity retention of lithium ion batteries cycled at elevated temperature (60 °C). Ex situ surface analysis (XPS and FTIR) of the electrodes suggests that generation of poly(methylene ethylene carbonate) on the anode surface results in a anode SEI with superior thermal stability and alters the surface chemistry of the cathode. MEC is a promising thermal stabilizing additive for lithium ion batteries.

References

[1] K. Xu, Chem. Rev. 104 (2004) 4304.
[2] C. Campion, W. Li, W.B. Euler, B.L. Lucht, B. Ravdel, J. Dicarlo, R. Gitzendanner, K.M. Abraham, Electrochem. Solid State Lett. 7 (2004) A194.
[3] M. Broussely, S. Herreyre, P. Biensan, P. Kasztejna, K. Nechev, R.J. Staniewicz, J. Power Sources 97–98 (2001) 13.
[4] M. Herstedt, D.P. Abraham, J.B. Kerr, K. Edstrom, Electrochem. Acta 49 (2004) 5097.
[5] M. Broussely, Ph. Biensan, F. Bonhomme, Ph. Blanchard, S. Herreyre, K. Nechev, R.J. Staniewicz, J. Power Sources 146 (2005) 90.
[6] L.E. Ouatani, R. Dedryvere, C. Siret, P. Biensan, S. Reynaud, P. Iratcabal, D. Gonbeau, J. Electrochem. Soc. 156 (2009) A103.
[7] D. Aurbach, K. Gamolsky, B. Markovsky, Y. Gofer, M. Schmidt, U. Heider, Electrochim. Acta 47 (2002) 1423.
[8] M.C. Smart, B.L. Lucht, B.V. Ratnakumar, J. Electrochem. Soc. 155 (2008) A557.
[9] W. Li, A. Xiao, B.L. Lucht, M.C. Smart, B.V. Ratnakumar, J. Electrochem. Soc. 155 (2008) A648.
[10] W. Xu, P. Bolomey, M.W. Payne, Patent Appl. US 2009/0017386.
[11] M. Kotato, S. Kinoshita, Patent Appl. US 2009/0253045.
[12] H. Yamamoto, H. Yamamoto, M. Nishiyama, H. Imagawa, M. Nishizawa, Tetrahedron. Lett. 47 (2006) 8369.